

Single-plane-wave Larkin-Ovchinnikov-Fulde-Ferrell state in BCS–Bose-Einstein condensation crossover

Yan He, Chih-Chun Chien, Qijin Chen and K. Levin

James Franck Institute and Department of Physics, University of Chicago, Chicago, Illinois 60637

(Dated: 18th December 2019)

We study the single-plane-wave Larkin-Ovchinnikov-Fulde-Ferrell (LOFF) states for BCS–Bose-Einstein condensation (BEC) crossover at general temperatures T . Because we include the important effects of non-condensed pairs, our $T \neq 0$ phase diagrams are different from those reported in earlier work. We find that generalized LOFF phases may be the ground state for a wide range of (weak through moderately strong) interactions, including the unitary regime. However, these LOFF phases are readily destroyed by non-zero T .

PACS numbers: 03.75.Hh, 03.75.Ss, 74.20.-z

cond-mat/0610274

Recent atomic physics discoveries in the field of ultracold polarized [1, 2, 3] fermionic superfluids have important implications in color superconducting quark matter as well as in dense nuclear matter [4, 5, 6]. Moreover, there has been a long standing interest from the condensed matter community [7] in observing the very elusive Larkin-Ovchinnikov-Fulde-Ferrell (LOFF) [8] states of a polarized superfluid. Here condensation of Cooper pairs takes place at one or more non-zero momenta \mathbf{q}_i . These cold gases possess a remarkable flexibility in which they can be polarized as well as studied with variable attractive interaction. This provides an additional mechanism for (possibly) tuning in the various LOFF phases as one changes the s -wave two-body scattering length a from positive in the Bose-Einstein condensation (BEC) regime to negative (BCS).

Thus far, experiments [1, 2, 3] have focused on the unitary scattering regime, midway from BCS to BEC. Bogoliubov-de Gennes (BdG)- based theories [9, 10] suggest that at unitarity the ground state, within a trap, has LOFF characteristics. By contrast, theories of the zero temperature, T , phase diagram for a homogeneous system suggest that one particular member of the LOFF class – corresponding to the single plane wave LOFF state (hereafter called LOFF1)– only appears in a narrow regime near the BCS endpoint [11]. A critical component which needs to be injected into this controversy is the nature of the stability criteria [12, 13, 14, 15] which is, similarly, under lively debate.

The goal of this paper is to clarify these issues by addressing BCS-BEC crossover at general T for the LOFF1 state in a homogeneous system. We characterize the “existence regime” (where solutions exist) and the “stability regime” (where solutions are stable) in a series of phase diagrams. Our results are quantitatively different from those in Ref. [16] in part because we implement a highly numerical procedure to solve all coupled equations directly at fixed total particle number N_σ . In *qualitative* agreement with Ref. [16] the *stable* LOFF1 state is primarily restricted to a regime near the BCS endpoint, although it does overlap unitarity for a narrow range of high polarizations. We show that the LOFF1 existence regime is considerably broader and is directly associated [17] with the phase space region where there is negative superfluid density [12, 18] in the $\mathbf{q} = 0$ or Sarma state [19]. Here it is likely that a LOFF phase of one form or another will be stable, although

it may be something more complex [7, 20] than LOFF1.

Our central phase diagram in the T vs p plane should be of particular interest to experimentalists who are currently creating plots of this nature. It can be contrasted with that obtained in Ref. [21] in which temperature was introduced in a fashion following the original Noziers–Schmitt-Rink (NSR) [22] scheme. Here, unlike Ref. [21] we choose to include T in a manner which is fully consistent with the very extensive literature [9, 10, 11, 12] on the ground state of these polarized superfluids.

We introduce $T \neq 0$ following a T -matrix scheme, and restrict our attention to the superfluid phase. This T -matrix represents the propagator for non-condensed pairs and is given by $t^{-1}(P) = U^{-1} + \chi(P)$ where χ is the pair susceptibility and $U < 0$ is the pairing interaction strength. For atomic Fermi gases, we assume an s -wave contact interaction. There are strong similarities between $t(P)$ and the Hartree-Fock approximation to the particle-hole susceptibility which involves the usual Lindhard function and on-site repulsion. These Hartree-Fock theories are used to establish whether ferro- or antiferromagnetic order will arise. Here we consider a very similar competition between Sarma and LOFF1 states. The relevant $\chi(P)$ necessarily involves the self consistently determined fermionic gap parameter $\Delta(T)$ and chemical potential $\mu(T)$. Importantly at and below T_c the chemical potential for the *pairs* (μ_{pair}) must be zero and this BEC condition on $t(P)$, thereby, determines $\Delta(T)$.

The pair susceptibility for LOFF1 condensates in which momentum \mathbf{k} pairs with $-\mathbf{k} + \mathbf{q}$, (for, as yet undetermined \mathbf{q}) may readily be written down [20]. We first introduce the fermionic chemical potentials for the two spin states $\mu = (\mu_\uparrow + \mu_\downarrow)/2$ and $h = (\mu_\uparrow - \mu_\downarrow)/2$, and $\epsilon_{\mathbf{k}} = \mathbf{k}^2/2m$, $\xi_{\mathbf{k}} = \epsilon_{\mathbf{k}} - \mu$, where μ_σ is the chemical potential for spin $\sigma = \uparrow, \downarrow$. It is useful to also define $E_{\mathbf{k}\mathbf{q}} = \sqrt{\xi_{\mathbf{k}\mathbf{q}}^2 + \Delta^2}$, with $\xi_{\mathbf{k}\mathbf{q}} = (\xi_{\mathbf{k}} + \xi_{\mathbf{k}-\mathbf{q}})/2$ and $\delta\epsilon_{\mathbf{k}} = (\epsilon_{\mathbf{k}} - \epsilon_{\mathbf{k}-\mathbf{q}})/2$. As in Ref. [23], we set the volume $V = 1$, $\hbar = k_B = 1$, and $P \equiv (i\Omega_l, \mathbf{p})$, where $\Omega_l = 2l\pi T$ is an even Matsubara frequency. Then the pair susceptibility $\chi(P)$ at the mean field level, after analytical continuation $i\Omega_l \rightarrow \Omega + i0^+$, is given by

$$\chi(P) = \sum_{\mathbf{k}} \left[u_{\mathbf{k}}^2 \frac{\bar{f}(E_{k\mathbf{q}} + \delta\epsilon_{\mathbf{k}}) + \bar{f}(\xi_{\mathbf{p}-\mathbf{k}}) - 1}{\Omega - \xi_{\mathbf{p}-\mathbf{k}} - (E_{k\mathbf{q}} + \delta\epsilon_{\mathbf{k}})} + v_{\mathbf{k}}^2 \frac{\bar{f}(\xi_{\mathbf{p}-\mathbf{k}}) - \bar{f}(E_{k\mathbf{q}} - \delta\epsilon_{\mathbf{k}})}{\Omega - \xi_{\mathbf{p}-\mathbf{k}} + (E_{k\mathbf{q}} - \delta\epsilon_{\mathbf{k}})} \right], \quad (1)$$

which, as $\mathbf{q} \rightarrow 0$, goes over smoothly to its counterpart in the Sarma phase. Here the coherence factors $u_{\mathbf{k}}^2, v_{\mathbf{k}}^2 = (1 \pm \xi_{k\mathbf{q}}/E_{k\mathbf{q}})/2$ and we define $\bar{f}(x) = [f(x-h) + f(x+h)]/2$, where $f(x)$ is the Fermi distribution function. The BEC condition, $U^{-1} + \chi(0, \mathbf{q}) = 0$, leads to the gap equation which, when written in terms of the scattering length a , is of the standard form in the literature

$$-\frac{m}{4\pi a} = \sum_{\mathbf{k}} \left[\frac{1 - 2\bar{f}(E_{k\mathbf{q}})}{2E_{k\mathbf{q}}} - \frac{1}{2\epsilon_k} \right], \quad (2)$$

where we define $\bar{f}(x) \equiv [f(x-h+\delta\epsilon_{\mathbf{k}}) + f(x+h-\delta\epsilon_{\mathbf{k}})]/2$.

The number equations also depend on the quantity χ through a self energy involving $t(P)$; we show the details elsewhere [20] but summarize our final results which yield the standard equations in the literature

$$n = 2 \sum_{\mathbf{k}} \left[v_{\mathbf{k}}^2 + \frac{\xi_{k\mathbf{q}}}{E_{k\mathbf{q}}} \bar{f}(E_{k\mathbf{q}}) \right], \quad (3)$$

$$\delta n = \sum_{\mathbf{k}} \delta f(E_{k\mathbf{q}}), \quad (4)$$

where $n = n_{\uparrow} + n_{\downarrow}$ and $\delta n = n_{\uparrow} - n_{\downarrow}$, and the polarization $p \equiv \delta n/n$. Here we have defined $\delta f(x) = [f(x-h+\delta\epsilon_{\mathbf{k}}) - f(x+h-\delta\epsilon_{\mathbf{k}})]$. Finally, we determine \mathbf{q} by imposing an extremal condition on the pair susceptibility, $\left. \frac{\partial \chi(0, \mathbf{p})}{\partial \mathbf{p}} \right|_{\mathbf{p}=\mathbf{q}} = 0$. This condition, which turns out to be equivalent to requiring that there be no net current in this LOFF1 state, is given by

$$0 = \frac{1}{\Delta^2} \sum_{\mathbf{k}} \left\{ \frac{\mathbf{q}}{2} \left[\left(1 - \frac{\xi_{k\mathbf{q}}}{E_{k\mathbf{q}}} \right) - \frac{\xi_{k\mathbf{q}}}{E_{k\mathbf{q}}} \bar{f}(E_{k\mathbf{q}}) \right] + \left(\mathbf{k} - \frac{\mathbf{q}}{2} \right) \delta f(E_{k\mathbf{q}}) \right\}. \quad (5)$$

When this equation has a solution at $\mathbf{q} \neq 0$ we have a LOFF1 phase. There will always be a co-existing solution of the Sarma-type with $\mathbf{q} = 0$.

At $T \neq 0$, the parameter $\Delta(T)$ contains the contribution from both condensed (sc) and non-condensed (pg) pairs. We can show quite generally that below T_c , $\Delta^2(T) \equiv \Delta_{sc}^2(T) + \Delta_{pg}^2(T)$, where

$$\Delta_{pg}^2(T) = Z^{-1} \sum_{\mathbf{p}} b(\Omega_{\mathbf{p}}), \quad (6)$$

and $b(x)$ is the Bose distribution function. Here the pair dispersion is found to be $\Omega_{\mathbf{p}} \approx (\mathbf{p} - \mathbf{q})^2/2M^*$. Analytical expressions for M^* and Z are possible via an expansion of χ in small $(\mathbf{p} - \mathbf{q})$,

$$\chi(\Omega, \mathbf{p}) - \chi(0, \mathbf{q}) \approx Z \left[\Omega - \frac{(\mathbf{p} - \mathbf{q})^2}{2M^*} \right], \quad (7)$$

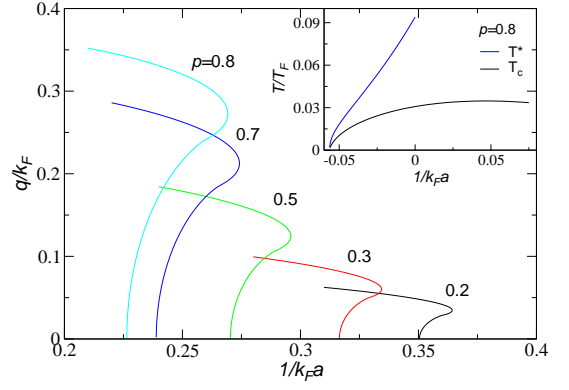


Figure 1: LOFF1 wavevector q as a function of $1/k_F a$ at $T = 0$ and for various p . Beyond the turning point, no LOFF1 state exists. The inset shows T_c and mean field $T_c^{MF} = T^*$ (pair formation temperature) at unitarity over respective stability regimes.

where $Z = \left. \frac{\partial \chi}{\partial \Omega} \right|_{\Omega=0, \mathbf{p}=\mathbf{q}}$ and $\frac{1}{2M^*} = - \left. \frac{1}{6Z} \frac{\partial^2 \chi}{\partial \mathbf{p}^2} \right|_{\Omega=0, \mathbf{p}=\mathbf{q}}$. The quantity χ contains everything one needs to know about zero as well as finite T . And our results for $T = 0$ reduce to the standard equations in the literature.

To demonstrate that a given LOFF1 solution to our self-consistent equations is stable, we introduce an effective thermodynamic potential for this superfluid state

$$\Omega = -\frac{\Delta^2}{U} + \sum_{\mathbf{k}} \left\{ (\xi_{k\mathbf{q}} - E_{k\mathbf{q}}) - T \ln(1 + \exp[-(E_{k\mathbf{q}} - h + \delta\epsilon_{\mathbf{k}})/T]) - T \ln(1 + \exp[-(E_{k\mathbf{q}} + h - \delta\epsilon_{\mathbf{k}})/T]) \right\}. \quad (8)$$

It is straightforward to verify that the above gap, number and zero-current equations are consistent with the variational conditions

$$\frac{\partial \Omega}{\partial \Delta} = 0; \quad -\frac{\partial \Omega}{\partial \mu} = n; \quad -\frac{\partial \Omega}{\partial h} = \delta n; \quad \frac{\partial \Omega}{\partial \mathbf{q}} = 0.$$

The stability condition requires that the symmetric number susceptibility matrix

$$M = \begin{pmatrix} \frac{DN}{D\mu} & \frac{DN}{Dh} \\ \frac{D\delta N}{D\mu} & \frac{D\delta N}{Dh} \end{pmatrix} \quad (9)$$

be positive definite [12, 13]. Here $\frac{D}{Dx} \equiv \frac{\partial}{\partial x} + \frac{\partial \Delta}{\partial x} \frac{\partial}{\partial \Delta} + \frac{\partial \mathbf{q}}{\partial x} \frac{\partial}{\partial \mathbf{q}}$, with $x = \mu, h$. To evaluate this matrix we note

$$\begin{aligned} \frac{DN}{D\mu} &= -\frac{\partial^2 \Omega}{\partial \mu^2} - \frac{\partial^2 \Omega}{\partial \Delta \partial \mu} \frac{\partial \Delta}{\partial \mu} - \frac{\partial^2 \Omega}{\partial q \partial \mu} \frac{\partial q}{\partial \mu}, \\ \frac{DN}{Dh} &= -\frac{\partial^2 \Omega}{\partial \mu \partial h} - \frac{\partial^2 \Omega}{\partial \Delta \partial h} \frac{\partial \Delta}{\partial h} - \frac{\partial^2 \Omega}{\partial q \partial h} \frac{\partial q}{\partial h} = \frac{D\delta N}{D\mu}, \\ \frac{D\delta N}{Dh} &= -\frac{\partial^2 \Omega}{\partial h^2} - \frac{\partial^2 \Omega}{\partial \Delta \partial h} \frac{\partial \Delta}{\partial h} - \frac{\partial^2 \Omega}{\partial q \partial h} \frac{\partial q}{\partial h}, \end{aligned} \quad (10)$$

where $\partial \Delta / \partial \mu$, $\partial q / \partial \mu$, $\partial \Delta / \partial h$, and $\partial q / \partial h$ can be easily derived by differentiating Eqs. (2) and (5) with respect to μ and h . It can be shown that the positive definiteness of M is equivalent to

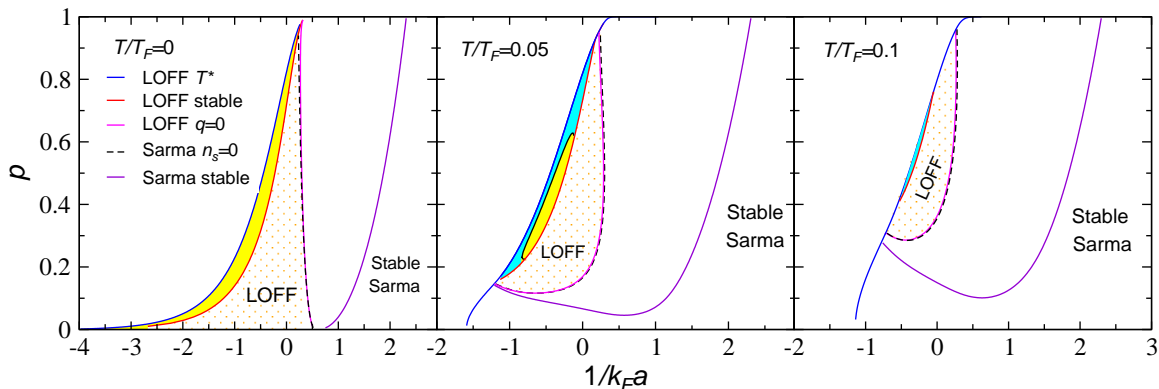


Figure 2: (Color online) Phase diagram in the p vs $1/k_F a$ plane for $T/T_F = 0, 0.05$, and 0.1 . The dotted region shows where LOFF1 state is unstable but some form of LOFF phase may be stable. The (yellow) light shaded region indicates the stable LOFF1 superfluid and the (cyan) darker shaded region the stable LOFF1 normal state.

$$\frac{\partial^2 \Omega}{\partial \Delta^2} \frac{\partial^2 \Omega}{\partial q^2} - \left(\frac{\partial^2 \Omega}{\partial \Delta \partial q} \right)^2 > 0, \quad (11)$$

In Ref. [11], the authors determined the stability line in the μ, h plane and claimed [24] that this line is preserved under a mapping to fixed $N, \delta N$. However, there appear to be significant differences between our stability lines (determined directly in the $N, \delta N$ plane) and theirs. Here, unlike Ref. [11], we did not investigate global energy minimization (at $T = 0$).

Equations (2)-(6) were solved numerically to establish the existence regime for LOFF1 solutions. Figure 1 shows a plot of the behavior of the LOFF1 wavevector \mathbf{q} as a function of $1/k_F a$, and at $T = 0$, for various polarizations p . Here $E_F = k_B T_F = \hbar^2 k_F^2 / 2m$ is defined as the Fermi energy of an unpolarized, noninteracting Fermi gas of density n . For each value of p a turning point, $(1/k_F a)_{max}$, is visible beyond which we can not find LOFF1 solutions. At finite T the analogous curves (not shown) quickly become monotonically decreasing so that $(1/k_F a)_{max}$ corresponds to $\mathbf{q} = 0$; thus the system smoothly transforms to the Sarma state.

The inset in Fig. 1 shows the behavior of T_c and its mean field counterpart $T^* = T_c^{MF}$ as a function of $1/k_F a$ near unitarity and for $p = 0.8$. It can be seen that there is a considerable difference between T_c and T_c^{MF} showing that pair fluctuation effects (via $\Delta_{pg} \neq 0$) are very important in the LOFF1 phase, just as seen elsewhere [18]. In contrast to the behavior of the Sarma phase at unitarity, in the LOFF1 state, superfluidity extends over the range of temperatures from T_c down to $T = 0$.

We turn to Fig. 2 beginning with the left panel ($T = 0$) and the nearly vertical line which is determined from $(1/k_F a)_{max}$. This provides a bound on the existence region for our numerically obtained LOFF1 solutions. Essentially on top of this nearly vertical line is the locus of points to the left of which the superfluid density for the Sarma state $n_s^{Sarma}(0)$ is negative. That these two lines coincide reinforces earlier work [17]: providing one considers a second order transition between generalized LOFF and Sarma states, the boundary line for the existence of *all* LOFF states is determined by $n_s^{Sarma} = 0$. We indicate by the dotted background in Fig. 2

where we have the possibility of superfluidity with multiple nonzero \mathbf{q} 's. It should be noted that this existence regime for generalized LOFF states is relatively wide at $T = 0$, importantly including unitarity. The shaded region in Fig. 2 results from applying the stability criteria associated with the positivity of the matrix M in Eq. (9). The non-vertical line to the right in this first panel marks the onset point for a stable Sarma phase.

This phase diagram evolves with temperature as shown by the other two panels in Fig. 2. In the middle and right panels we have distinguished between normal and superfluid LOFF1 states by using darker and lighter shaded regions respectively. At the highest T , for the panel on the right, there is only a sliver of stable LOFF1 which corresponds to a normal (pseudogapped) phase. It should be noted that the size of the existence region for generalized LOFF solutions quickly decreases as temperature is raised. This is related to the fact that the n_s^{Sarma} rapidly becomes non-negative as T increases from zero.

Figure 3 represents a particularly convenient way of presenting our results. For the trapped case, experimental studies [1, 2, 3] are in the process of mapping out this phase diagram in the $p-T$ plane at unitarity. From left to right, the three panels correspond to unitarity, and the BCS and BEC sides (close to resonance), respectively. Also shown here is the region where we have a stable Sarma state. This appears only at intermediate temperatures [18], when the superfluid density (which is negative at $T = 0$ for all 3 cases) is driven positive. Note that our $p-T$ phase diagram is different from that in Ref. [21], which is based on a different but unspecified ground state. Indicated in all three panels are the (dotted) regions where generalized LOFF states may exist, and the (shaded) regimes where the LOFF1 phase is stable. As in Fig. 2, the light shaded region corresponds to the superfluid LOFF1 phase, and the dark shaded region to the normal LOFF1 phase with a pseudogap. It is evident that, for these $1/k_F a$ values, a stable LOFF1 phase exists only at relatively high p and low T . This is to be contrasted with the stable Sarma superfluid which exists only at low p and intermediate T . Using this figure, one can compare the transition temper-

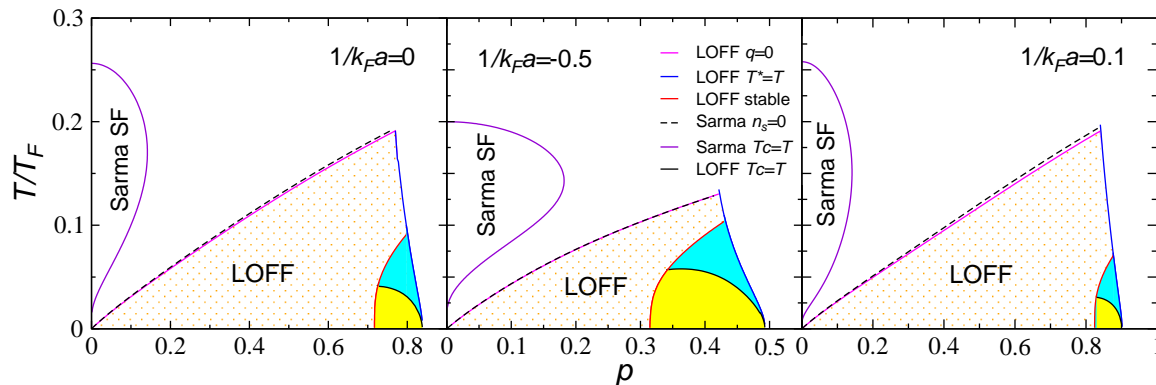


Figure 3: (Color online) Phase diagram in the $p-T$ plane for unitary (left), near BCS (middle) and near-BEC (right). The dotted region shows where LOFF1 state is unstable but stable generalized LOFF phases may in principle exist. The (yellow) light shaded region is the LOFF1 superfluid, and the (cyan) darker shaded region is the LOFF1 normal state.

atures for the LOFF1 and Sarma phases. For the latter, T_c is read off as the upper transition temperature in the 3 plots. (The lower T_c is where $n_s^{\text{Sarma}}(T)$ changes sign and the order parameter vanishes). It can be seen that the transition temperatures for the LOFF1 phase are very low compared to their counterparts in the Sarma phase.

In summary, in this paper we have addressed homogeneous systems and mapped out the LOFF1 phase diagram at general T . We have shown that LOFF1 phases are more stable near unitarity at sufficiently high p than alternative Sarma states. Since it is generally expected [7] that LOFF states with multiple values of \mathbf{q} are more stable than the simplest LOFF1 states, we argue that quite possibly there exist stable generalized LOFF ground states throughout most (but perhaps not all) of the dotted regions shown in Figs. 2 and 3; this corresponds to where the Sarma phase has negative superfluid density. Our

results support previous BdG-based approaches [9, 10] which argue that the ground state at unitarity is a generalized LOFF phase. In a trap configuration, one might expect that, since we find the LOFF1 phase is stable at relatively high p , generalized LOFF phases should appear in the neighborhood of the condensate edge, as also found in earlier work [9, 10]. However, in contrast to Ref. [9], we have addressed systematic LOFF1 stability criteria and, moreover, find that the size of the stability region for the LOFF1 state and the size of the existence region for general LOFF phases very quickly diminish with T . Finally, our self consistent calculations indicate very low T_c in the LOFF1 state as compared with previous estimates in the literature [9], which ignored the effects of noncondensed pairs.

This work was supported by NSF PHY-0555325 and NSF-MRSEC Grant No. DMR-0213745.

-
- [1] M. W. Zwierlein, A. Schirotzek, C. H. Schunck, and W. Ketterle, *Science* **311**, 492 (2006).
 - [2] G. B. Partridge, W. Li, R. I. Kamar, Y. A. Liao, and R. G. Hulet, *Science* **311**, 503 (2006).
 - [3] M. W. Zwierlein, C. H. Schunck, A. Schirotzek, and W. Ketterle, *Nature (London)* **442**, 54 (2006).
 - [4] W. V. Liu and F. Wilczek, *Phys. Rev. Lett.* **90**, 047002 (2003).
 - [5] M. M. Forbes, E. Gubankova, W. V. Liu, and F. Wilczek, *Phys. Rev. Lett.* **94**, 017001 (2005).
 - [6] R. Casalbuoni and G. Nardulli, *Rev. Mod. Phys.* **76**, 263 (2004).
 - [7] C. Mora and R. Combescot, *Phys. Rev. B* **71**, 214504 (2006).
 - [8] P. Fulde and R. A. Ferrell, *Phys. Rev.* **135**, A550 (1964); A. I. Larkin and Y. N. Ovchinnikov, *Zh. Eksp. Teor. Fiz.* **47**, 1136 (1964) [*Sov. Phys. JETP* **20**, 762 (1965)].
 - [9] K. Machida, T. Mizushima, and M. Ichioka, *Phys. Rev. Lett.* **97**, 120407 (2006).
 - [10] J. Kinnunen, L. M. Jensen, and P. Torma, *Phys. Rev. Lett.* **96**, 110403 (2006).
 - [11] D. E. Sheehy and L. Radzihovsky, *Phys. Rev. Lett.* **96**, 060401 (2006).
 - [12] C. H. Pao, S. T. Wu, and S. K. Yip, *Phys. Rev. B* **73**, 132506 (2006).
 - [13] E. Gubankova, A. Schmitt, and F. Wilczek, *Phys. Rev. B* **74**, 064505 (2006).
 - [14] Q. J. Chen, Y. He, C.-C. Chien, and K. Levin (2006), e-print cond-mat/0608454.
 - [15] D. E. Sheehy and L. Radzihovsky (2006), e-print cond-mat/0608172.
 - [16] D. E. Sheehy and L. Radzihovsky (2006), e-print cond-mat/0607803.
 - [17] L. Y. He, M. Jin, and P. F. Zhuang, e-print cond-mat/0606322.
 - [18] C.-C. Chien, Q. J. Chen, Y. He, and K. Levin, *Phys. Rev. Lett.* **97**, 090402 (2006).
 - [19] G. Sarma, *J. Phys. Chem. Solids* **24**, 1029 (1963).
 - [20] Q. J. Chen, H. Yan, C.-C. Chien, and K. Levin (2006), preprint, cond-mat/0608662.
 - [21] M. Parish, F. Marchetti, A. Lamacraft, and B. Simons (2006), e-print cond-mat/0605744.
 - [22] P. Nozières and S. Schmitt-Rink, *J. Low Temp. Phys.* **59**, 195 (1985).
 - [23] C.-C. Chien, Q. J. Chen, Y. He, and K. Levin, *Phys. Rev. Lett.* **97**, 090402 (2006).
 - [24] L. Radzihovsky, private communication.